Dalton Transactions

ROYAL SOCIETY OF CHEMISTRY

PAPER

View Article Online
View Journal | View Issue

Cite this: *Dalton Trans.*, 2025, **54**, 14396

Exploring the effect of copper on the bioactivity of 8-quinolines: an *in vitro* and *in vivo* study

Alessia Sambugaro, [a] Riccardo Po,[a] Martina Lorenzetto,[b] Rebecca Ceolin,[b] Giuditta Palmerston,[a,b] Erik Murador,[a] Laura Cifalinò, [c] Giulia Annesi, [d] Valeria Scalcon, [d] Chiara Nardon *[a] and Valentina Oliveri *[c]

Current anticancer therapy is challenged by the adaptability and resistance of tumor cells as well as limited drug selectivity that causes severe side effects. The scientific community maintains high interest in metal-based chemotherapeutic agents due to their unique interactions with cancer cells, potentially overcoming resistance mechanisms and exploiting the physiopathology of the tumour tissues. Copper, in particular, plays a dual role in cancer, both facilitating tumor progression and triggering cuproptosis, a copper-induced cell death mechanism. A better understanding of these processes has revived interest in copper-based therapies as a promising strategy against cancer. This work contributes to this field by investigating 8-aminoquinoline (**8AQ**) in combination with copper as an anticancer agent. Given its structural similarity to 8-hydroxyquinoline (8HQ), a known copper ionophore, we investigated whether the presence of Cu could influence its antitumor activity. For comparison purposes, we also studied 8-nitroquinoline (**8NQ**), which binds copper with lower affinity but may undergo selective reduction in those tumor tissues overexpressing the nitroreductase enzyme. **8AQ** alone exhibits poor anticancer activity (in the human cancer cell lines explored here: A549, HepG2, and HCT116), but in the presence of copper ions, its effectiveness nearly doubles. *In vivo* experiments on zebrafish (*Danio rerio*) embryos confirmed the *in vitro* results, highlighting no toxicity *in vivo* and no cytotoxicity *in vitro* for **8NQ** in parallel with stronger effects recorded with **8AQ** both alone and in combination with copper. Our chemical and biological findings provide valuable insights into the pharmacological profile of the **8AQ**–copper system, paving the way to further investigations and offering new experimental models to advance copper-based therapeutic strategies.

Received 13th June 2025,
Accepted 19th August 2025

DOI: 10.1039/d5dt01396h

rsc.li/dalton

Introduction

After cardiovascular diseases, cancer ranks as the second leading cause of death worldwide.[1,2] A variety of treatment approaches have been developed so far, including surgery, chemotherapy, radiation therapy, gene therapy, and immunotherapy.[3,4] However, the inherent complexity and adaptability of cancer cells, which can develop resistance,[5,6] create a pressing need for ongoing innovation, particularly in developing new agents to counteract this resistance. Among the various types of chemotherapy, metal-based agents still attract significant interest due to their potential to be more effective against certain tumour types.[7,8] Some of these agents may also exhibit selectivity towards some pathophysiological features of tumour cells, offering a more targeted approach to cancer treatment.[9] Metals, with their distinct chemical properties, can interact with cells in ways that organic molecules typically cannot replicate. In the context of oncology, this ability may allow metallodrugs to bypass resistance mechanisms that conventional treatments often face.

Copper is deeply involved in tumour growth and metastasis, a feature particularly noteworthy in most solid tumours. Cancer tissues often exhibit elevated copper levels, a phenomenon known as cuproplasia.[10–13] Copper plays a crucial role in promoting cancer progression through (i) the activation of signalling pathways like MAPK (Mitogen-Activated Protein Kinase), which is involved in cell growth, differentiation, and survival[14] and (ii) the modulation of the extracellular matrix (ECM) environment as one key copper-dependent enzyme, lysyl oxidase (LOX), involved in ECM remodelling, can facilitate the migration of tumour cells. LOX catalyses the crosslinking

[a]*Biomedical Chemistry Lab, Department of Biotechnology, University of Verona, Strada le Grazie 15, 37134 Verona, Italy*
[b]*Agrolab Italia Srl a socio unico, via Retrone 29/31, Altavilla Vic., Italy*
[c]*Biomedical Inorganic Chemistry Lab, Department of Chemical Sciences, University of Catania, v.le A. Doria 6, 95125 Catania, Italy.*
E-mail: valentina.oliveri@unict.it
[d]*Department of Biomedical Sciences, University of Padova, via Ugo Bassi 58/b, 35131 Padova, Italy*

of collagen and elastin fibres, which alters tissue stiffness and promotes a more favourable environment for cancer cell invasion and metastasis.[15,16]

Regarding the dual role of copper in cancer biology, on the one hand, as mentioned earlier, it can drive various processes that promote cancer development and metastasis, on the other hand, excess copper ions can activate a cell death mechanism known as cuproptosis,[17,18] effectively halting tumour progression. The accumulation of copper ions triggers the aggregation of lipoylated dihydrolipoamide *S*-acetyltransferase (DLAT), a pivotal component of the pyruvate dehydrogenase complex, which links glycolysis to the tricarboxylic acid cycle. The aggregation of DLAT induces proteotoxic stress, ultimately leading to cell death. Furthermore, cuproptosis is characterized by the degradation of proteins containing iron–sulfur (Fe–S) clusters, which further disrupts cellular functioning.[19,20]

Historical observations indicated that excessive copper levels could trigger cancer cell death, with ionophores suspected to facilitate this process.[21,22] However, the lack of clarity surrounding the mechanism of action, which was later named cuproptosis, initially dampened enthusiasm. Today, with advancing knowledge, copper-based therapies are emerging as a promising avenue for effectively combating tumours.

Among the recognized copper ionophores that cause cell death, elesclomol (ES), dithiocarbamates (DTCs), and 8-hydroxyquinolines (8HQs) stand out.[22,23] These compounds have also been studied by us both in their native form and functionalized form; functionalization enhances may enhance their selectivity for tumour cells.[24–27] In this context, given the structural similarity between the 8HQ and 8-aminoquinoline (**8AQ**) scaffolds, we perceived the value in studying the combination of copper with **8AQ** (Fig. 1 inset) as a new anticancer strategy. As a comparison, in this work, we also studied the 8-nitroquinoline derivative (**8NQ**, Fig. 1 inset), which cannot bind with Cu^{2+} with the same affinity as **8AQ**. However, the nitro counterpart could undergo selective conversion into the amino derivative in tumour tissues that exhibit overexpression of tumour-specific nitroreductase enzymes; thus, it could act as a prodrug.[28] Besides studying the complex species of these compounds, we investigated their interaction with glutathione (GSH) and their effects on three human cancer cell lines (A549, HepG2 and HCT116). The evaluation of the capability to pass across membranes (log *P* determination) was followed by the *in vivo* toxicological studies carried out on zebrafish embryos (*Danio rerio*), as very few copper-based systems have been studied in this animal model so far, mainly for purposes other than oncological ones.[29–34]

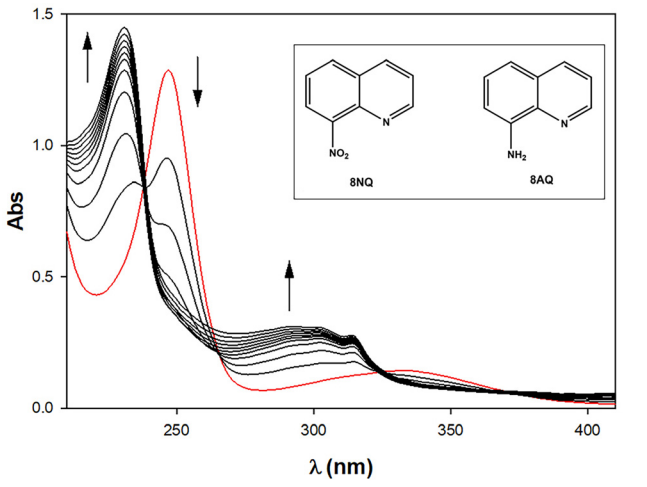

Fig. 1 UV-Vis titration of Cu^{2+} (0–2 mol equiv.) into a solution of **8AQ** at pH 7.4 (0.01 M MOPS/EtOH 70 : 30). The UV-vis spectrum of **8AQ** alone is highlighted in red. C_{8AQ} = 5.0 × 10^{-5} M. The inset shows the chemical structures of 8-aminoquinoline (**8AQ**) and 8-nitroquinoline (**8NQ**).

Results and discussion

8AQ, 8NQ and their corresponding copper complexes

Before evaluating copper complexation by the two quinolines, their lipophilic properties were evaluated. The *n*-octanol/water partition coefficient (log *P*), a useful parameter in pharmaceutical development, was experimentally determined by the shaking-flask method.[35–38] **8NQ** proved to be more hydrophobic than **8AQ**, with log *P* values of 1.72 ± 0.02 and 1.30 ± 0.05, respectively. The latter agrees with *in silico* defined data (log *P* = 1.38, obtained using the Molinspiration Cheminformatics 2024 online software tool).[39]

The formation of coordination compounds between copper and the two organic molecules, **8AQ** and **8NQ**, was studied in solution under conditions as close as possible to physiological ones. A small amount of organic solvent was nevertheless required to prevent precipitation of the complexes. The positive-ion mode ESI-MS spectra of water solutions of **8AQ** and Cu^{2+} ions at pH 7.0 are shown in Fig. S1 and S2 (SI). When Cu^{2+} was allowed to react with **8AQ** at a 1 : 2 metal-to-ligand molar ratio, ESI-MS spectra of the reaction mixtures indicated the formation of complexes with metal-to-ligand stoichiometric ratios of 1 : 2 and 1 : 1. In addition to the pseudo-molecular $[M + H]^+$ ion of **8AQ** at *m*/*z* 145.1, intense cluster signals indicating the presence of copper are observed at *m*/*z* 206.1, 223.9, 251.9 and 350.1 (Fig. S3–S8). In particular, the peaks at *m*/*z* 206.1, 223.9, and 251.9 can be assigned to the CuL species (Table 1), formed by one **8AQ** molecule and one copper center with different coordinating molecules, such as water and ethanol (the stock solution of **8AQ** was prepared in ethanol). The peak at *m*/*z* 350.1 is attributed to a complex formed by two **8AQ** molecules and one copper ion (calculated *m*/*z* ratio for the molecular composition $CuC_{18}H_{15}N_4$, Table 1).

The mass spectra of **8NQ**, both alone and in the presence of copper, showed no significant difference (also in the presence of an excess of copper ions). Only the peaks corresponding to the proton and sodium adducts of **8NQ** were detected, with *m*/*z* values of 175.1 and 196.9, respectively (Fig. S9 and S10). The mass spectra showed no evidence of complex formation between **8NQ** and Cu^{2+}, clearly indicating, as expected, an

Table 1 ESI-MS characterization of **8AQ**, **8NQ**, GSH solution and their mixtures with copper ions at pH 7.0

Sample	Species	Assignment	Calcd	Found	Rel. Abd.
8AQ $C_9H_8N_2$ (L)	$[L + H]^+$	$C_9H_9N_2$	145.1	145.1	100%
8AQ–Cu^{2+}	$[L + H]^+$	$C_9H_9N_2$	145.1	145.1	68%
	$[Cu^{II}L–H]^+$	$CuC_9H_7N_2$	206.0	206.1	52%
	$[Cu^{II}L + H_2O–H]^+$	$CuC_9H_9N_2O$	224.0	223.9	100%
	$[Cu^{II}L + C_2H_6O–H]^+$	$CuC_{11}H_{13}N_2O$	252.0	251.9	54%
	$[Cu^{II}L_2–H]^+$	$CuC_{18}H_{15}N_4$	350.1	350.1	26%
8NQ $C_9H_6N_2O_2$ (L)	$[L + H]^+$	$C_9H_7N_2O_2$	175.1	175.1	100%
	$[L + Na]^+$	$C_9H_6N_2O_2Na$	197.0	196.9	9%
8NQ–Cu^{2+}	$[L + H]^+$	$C_9H_7N_2O_2$	175.1	175.1	100%
	$[L + Na]^+$	$C_9H_6N_2O_2Na$	197.0	196.9	10%
GSH	$[2GSH + H]^+$	$C_{20}H_{35}N_6O_{12}S_2$	615.2	615.1	100%
8AQ-Cu^{2+}-GSH 1 : 1 : 2	$[L + H]^+$	$C_9H_9N_2$	145.1	145.1	100%
	$[Cu^{II}L + H_2O–H]^+$	$CuC_9H_9N_2O$	224.0	223.9	17%
	$[Cu^{II}L_2–H]^+$	$CuC_{18}H_{15}N_4$	350.1	350.2	12%
	$[GSSG + H]^+$	$C_{20}H_{33}N_6O_{12}S_2$	613.2	613.1	11%
	$[GSSG + Na]^+$	$C_{20}H_{32}N_6O_{12}S_2Na$	635.1	635.1	16%
	$[CuGSSG–H]^+$	$CuC_{20}H_{31}N_6O_{12}S_2$	674.1	674.0	17%
	$[CuGSSG + Na–2H]^+$	$CuC_{20}H_{30}N_6O_{12}S_2Na$	696.1	696.1	45%
	$[CuGSSG + K–2H]^+$	$CuC_{20}H_{30}N_6O_{12}S_2K$	712.0	712.1	25%
	$[CuGSSG + C_2H_6O–H]^+$	$CuC_{22}H_{35}N_6O_{13}S_2$	718.1	718.0	20%
	$[CuGSSG + Na + K–3H]^+$	$CuC_{20}H_{29}N_6O_{12}S_2KNa$	734.0	734.0	18%

extremely low affinity of **8NQ** for copper. To further demonstrate the lower affinity of **8NQ** for Cu^{2+} compared to that of **8AQ**, competition experiments were carried out. Mass spectra of mixtures containing **8AQ**, **8NQ**, and Cu^{2+} were acquired (Fig. S11). The spectra consistently showed peaks corresponding to Cu–**8AQ** complexes, even in the presence of an excess of **8NQ**. No peaks attributable to copper–**8NQ** species were observed in any of the spectra, indicating that **8NQ** does not effectively compete with **8AQ** for Cu^{2+} coordination under the tested conditions.

The formation of copper complex species of **8AQ** and **8NQ** was also monitored by UV-Vis spectrophotometry. The spectrum of **8AQ** recorded in MOPS (3-(*N*-morpholino)propanesulfonic acid)/EtOH shows two intense bands at 247 nm and 333 nm, corresponding to π–π* and n–π* transitions, respectively.[40]

The protonation state of the compounds under physiological conditions determines their solubility and ability to cross cell membranes. The pK_a of the **8AQ** moiety was determined by monitoring changes in the UV/Vis spectrum. Absorbance measurements at 246 nm (λ_{max} under basic conditions) and 260 nm (λ_{max} under acidic conditions) were plotted against pH to calculate the pK_a. For **8AQ**, the analysis revealed a single pK_a value of 4.09, consistent with the value reported by Martell and Smith.[41] The electronic spectra of the deprotonated form of **8AQ** are characterized by a main absorption band centered at 247 nm, and a weak and broad absorption band at 333 nm. The protonation of **8AQ** causes a red shift and a decrease in absorbance of the higher-energy electronic transitions. The relatively low pK_a of **8AQ** compared to that of quinoline can be attributed to the intramolecular hydrogen bonding between the amino group ($–NH_2$) and the nitrogen atom in the quinoline ring. The distribution diagram of the protonated species suggests that under our experimental conditions (MOPS/EtOH 70 : 30), **8AQ** predominantly exists in its neutral form. Upon the addition of copper ions, the UV spectrum of **8AQ** underwent significant changes, pointing out the formation of the complex species (Fig. 1). Following the titration of **8AQ** with a Cu^{2+} solution, the intensity of the peaks at 247 and 333 nm noticeably decreased, while the band maxima at 231 and 293 nm exhibited a clear increase in absorbance with rising copper concentration. The solid-state structure of the copper–8-aminoquinoline (**8AQ**) complex with a 1 : 2 metal-to-ligand ratio (ML_2) was determined by single-crystal X-ray diffraction and reveals a distorted octahedral geometry.[42] In this structure, each **8AQ** molecule acts as a bidentate ligand, coordinating the copper(II) center through the pyridine nitrogen and the amino nitrogen atoms. The distortion of the octahedral geometry is attributed to a pronounced Jahn–Teller effect, which leads to elongation along the axial axis. The two **8AQ** ligands occupy the equatorial plane, while the axial positions are typically filled by weakly bound water molecules or anions such as chloride or nitrate.

Based on our experimental data in solution, it is reasonable to propose a similar coordination environment for the ML_2 species, with two **8AQ** molecules acting as bidentate ligands through the same donor atoms observed in the solid-state structure. In contrast, in the ML species, only one **8AQ** molecule is coordinated to the metal center in a bidentate manner, and the remaining coordination sites are most likely occupied by water molecules.

In the absorption spectrum of **8NQ**, two intense bands are observed at 216 nm and 300 nm (Fig. S12). These bands are

characteristic of aromatic compounds like **8NQ** and can be attributed to $\pi \rightarrow \pi^*$ and $n \rightarrow \pi^*$ electronic transitions, respectively, typical of aromatic systems containing functional groups such as the nitro group.[43] Furthermore, the addition of one equivalent of copper did not lead to significant changes in the UV-Vis spectrum (Fig. S12), suggesting a much lower affinity of **8NQ** for copper ions compared to that of **8AQ**. This behavior is consistent with the data obtained from ESI-MS analysis. Similar to the mass spectrometry experiments, UV–vis competition studies were also carried out. The spectrum of the **8AQ**–Cu^{2+} complex remains unchanged upon the addition of either one or two equivalents of **8NQ**, after subtraction of the absorbance contribution from free **8NQ**. These findings confirm that **8AQ** exhibits a significantly stronger affinity for Cu^{2+} than **8NQ** under the conditions tested.

Interaction with GSH

Glutathione (γ-glutamyl–cysteinyl–glycine, GSH) is the main low-molecular-weight thiol in mammalian cells, with concentrations in the millimolar range.[44] The reduced/oxidized glutathione (GSH/GSSG) couple is a central regulator of redox homeostasis in animal cells. Under normal conditions, GSH predominates in its reduced form[45] and is involved in several cellular functions: it controls protein thiol oxidation, defends against oxidative stress, and supports metal detoxification.[46,47]

Due to its essential role in cell survival, GSH metabolism is a significant target for therapeutic interventions, particularly in oncology. A reduction in GSH levels has been linked to the onset of diseases such as cancer, cardiovascular conditions, and neurodegenerative disorders, while an increase in GSH has been associated with cancer growth and resistance to chemotherapy.[48,49] GSH also counteracts and inhibits copper-induced cuproptosis.[50] These effects make GSH depletion a promising strategy, especially in combination treatments. GSH acts as an intracellular reducing agent for Cu^{2+} ions and even trace amounts of Cu^{2+} can efficiently lead to GSH oxidation, forming GSSG.[51] In light of these considerations, an interaction between the copper complex of **8AQ** and GSH is highly probable. Consequently, we aimed to investigate the nature of the interaction between these systems.

The reaction of the Cu^{2+}–**8AQ** species with GSH in the presence of atmospheric oxygen was initially monitored by electronic spectrophotometry. The addition of 1 equivalent of GSH to the sample containing Cu^{2+}–**8AQ** at pH 7.4, under aerobic conditions, resulted in an immediate decrease of the band at 231 nm, accompanied by an increase of absorbance at 247 nm. This effect clearly suggests that the Cu^{2+}–**8AQ** complex species decreased in concentration while the concentration of the free ligand increased (Fig. 2). The addition of two equivalents of GSH resulted in the complete release of copper. Notably, the UV-Vis spectrum of the **8AQ**–Cu^{2+}–GSH 1 : 1 : 2 solution closely matches that of free **8AQ** at the same concentration, demonstrating a near-perfect overlap (Fig. 2). To better understand the interaction, the mass spectra of the Cu^{2+}–**8AQ** complex in the presence of 2 equivalents of GSH were also acquired (Table 1).

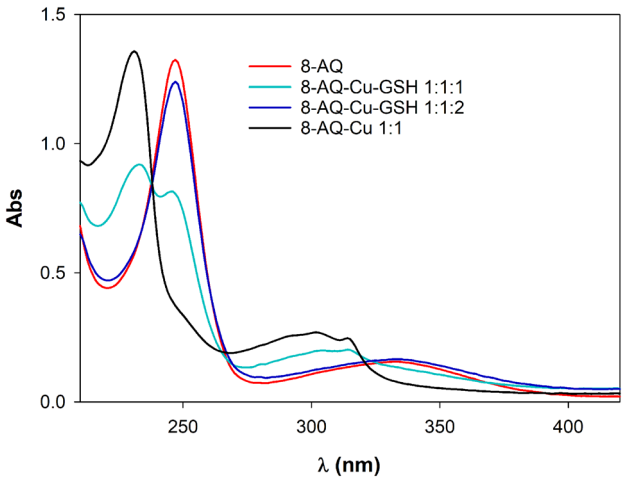

Fig. 2 UV-Vis spectra of **8AQ** alone and the mixtures **8AQ**-Cu^{2+} 1 : 1, **8AQ**-Cu^{2+}-GSH 1 : 1 : 1, and **8AQ**-Cu^{2+}-GSH 1 : 1 : 2 at pH 7.4 (0.01 M MOPS/EtOH 70 : 30). $C_{8AQ} = 5.0 \times 10^{-5}$ M.

The reaction mixture was analyzed by ESI-MS (with a positive detection mode, Fig. S13) soon after the GSH addition to the solution of the complex Cu^{2+}–**8AQ**. Compared to the Cu^{2+}–**8AQ** solution, an increase in the intensity of the protonated derivative of the ligand (m/z = 145.1) was observed in the solution which supports the demetallation of Cu^{2+}–**8AQ** after the reduction of copper by GSH. Additionally, a significant decrease in the relative intensity of the peaks at m/z 223.9 (from 100% to 17%) and 350.2 (from 26% to 12%) was identified, corresponding to the CuL and CuL_2 species, respectively (L = **8AQ**). Furthermore, the peaks at 206.1 and 251.9, previously ascribed to the CuL species coordinated with either a water or ethanol molecule, were no longer detectable.

The mass spectrum revealed peaks at m/z 613.1 and 635.1, corresponding to the oxidized form of glutathione (GSSG) (Fig. S14 and S15). Oxidized glutathione formed complexes with Cu^{2+}, with the predominant species appearing at m/z 674.0 and 696.2 (Table 1 and Fig. S16–S18). By analyzing the shape of the peaks of the copper–glutathione complexes and comparing them with the theoretical distribution, it is possible to determine the proportion of Cu^{+} and Cu^{2+} ions bound to glutathione.

The peak at m/z 674.0 was clearly attributed to the $[^{63}Cu^{2+}$–GSSG–H$]^+$ ion, while the $[^{65}Cu^{2+}$–GSSG–H$]^+$ ion was detected at m/z 676.0. However, the presence of a small percentage of the $[^{63}Cu^{+}$–GSSG$]^+$ species could be hypothesized at m/z 675.0 comparing the relative peak height proportions with the theoretical one. To sum up, once oxidized, glutathione tends to react primarily with Cu^{2+} ions and to a lesser extent with Cu^{+} ions. Copper ions are more likely to be coordinated to amino and carboxyl groups rather than thiol/disulfide groups.[52] Notably, no peaks corresponding to the reduced form of glutathione (GSH) were detected. Under identical conditions, the mass spectrum of GSH alone exhibited a single peak at m/z 615.1 due to the dimer $[2GSH + H]^+$.

Taken together, these findings indicate that GSH underwent oxidation, leading to the reduction of copper. The **8AQ** ligand released the metal center, which was then sequestered by the oxidized glutathione (GSSG).

In vitro antiproliferative activity

The antiproliferative activity of **8AQ** and **8NQ** alone or in the presence of Cu^{2+} was evaluated against three human cancer cell lines—A549 (non-small cell lung cancer), HepG2 (hepatocellular carcinoma), and HCT116 (colorectal carcinoma). The selection of these cell lines is based on literature data, indicating that they exhibit higher copper levels compared to the corresponding normal cells.[10,13,53–55] Moreover, Arnal *et al.* observed that A549 cells are more sensitive to copper ion overload compared to HepG2 cells.[56] The cell lines were also chosen in light of studies indicating elevated expression levels of the nitroreductase enzyme in these tumor types.[57–59]

Notably, the obtained EC_{50} values highlight that **8NQ** is less cytotoxic compared to its reduced counterpart **8AQ**. No substantial differences are observed among the three cancer cell lines, suggesting that **8NQ** is not effectively converted into **8AQ** through nitroreductase activity in any of the models tested. Given that high NTR expression has been reported in these cell lines, and that HCT116 cells are generally considered more sensitive to the activation of nitroaromatic compounds than A549 cells,[59] it is possible that other intracellular factors may be limiting the activation of the system.

8AQ and **8NQ** were further investigated in the presence of copper ions, in order to assess the impact of metal coordination on their biological activity.

At first, different concentrations of copper alone (5, 10, 20, and 50 μM) were tested, showing no significant effect on cell viability. Therefore, subsequent tests were performed using a fixed copper concentration of 20 μM while evaluating a concentration gradient of the ligands (1, 2, 3, 4, and 8 equivalents relative to the copper concentration). Table 2 shows that the EC_{50} values for **8AQ** alone were higher compared to those observed when **8AQ** was combined with 20 μM copper ions. Thus, the *in situ*-formed Cu^{2+}–**8AQ** species exhibited a better anticancer activity compared to the ligand alone. The EC_{50} values reported in Table 2 are consistent, in terms of copper sensitivity, with the evidence discussed above indicating that the A549 cell line is more sensitive to copper ions than HepG2.[56] In contrast, the presence of copper did not markedly affect the activity of **8NQ**. A slight effect of copper is observed only in the HCT116 cell line, which, according to literature data, is expected to be the most sensitive to the reduction of nitroaromatic compounds.[59] From these observations, the following conclusions can be drawn: (1) the increased activity observed in the presence of **8AQ** and Cu^{2+} is attributable to the binding between copper and the compound and (2) **8NQ** is either not converted or significantly activated into **8AQ**, or, if it is, it fails to bind to and reach the copper, and therefore is unable to elicit a greater biological activity.

Table 2 EC_{50} (μM ± SD) values for each cell line, being the mean value from at least three independent 72 h experiments

	Cell line		
System	A549	HepG2	HCT116
8NQ	>200	>200	>200
Cu^{2+}–**8NQ**[a]	—	>200	173 ± 3.5
8AQ	143 ± 36	>200	170 ± 6.6
Cu^{2+}–**8AQ**[a]	68.1 ± 1.7	123.8 ± 6.5	111 ± 9.2
Cu^{2+}	>50	>50	>50

[a] The EC_{50} data here reported refer to the organic ligand.

It is worth noting that the DMEM cell culture medium, as formulated, can compete with **8AQ** for copper binding, as evidenced by UV-Vis spectra of the Cu^{2+}–**8AQ** system recorded in the presence of increasing concentrations of culture medium (Fig. S19). The spectra clearly reveal a progressive decrease in the absorbance of the Cu^{2+}–**8AQ** complex bands at 231 and 293 nm, along with the reappearance of the characteristic absorption bands of the free ligand **8AQ** at 243 and 247 nm. This suggests that a portion of the copper added to the culture medium binds to medium components, reducing the amount available for complexation with **8AQ**. Despite this competition, the co-administration of copper and **8AQ** results in a significantly enhanced biological effect, as demonstrated by a twofold decrease in the EC_{50} value compared to that with the ligand alone.

Upon entering tumor cells, the Cu^{2+}–**8AQ** complex likely reacts with intracellular glutathione (GSH), leading to its dissociation, as demonstrated by the interaction data presented in the previous section. Since co-administration of **8AQ** with copper results in significantly enhanced antiproliferative activity compared to that with **8AQ** alone, these findings strongly support an ionophoric role of **8AQ**. **8AQ** could facilitate the transport of copper into cells, where the metal could be released upon interaction with GSH. The resulting accumulation of copper ultimately leads to intracellular copper overload. This mechanism relies on similarities with known ionophores featuring 8HQ-based scaffolds.[22] In light of the previous considerations, and in analogy with data reported for 8-hydroxyquinolines,[22] the active species responsible for the ionophoric behavior toward copper is likely the Cu^{2+}–**8AQ** complex, with a 1 : 1 or 1 : 2 metal-to-ligand stoichiometry. In the former case, components of the medium are likely involved in the coordination sphere, resulting in a heteroleptic complex. Taken together, the obtained EC_{50} data are quite high, making values difficult to achieve locally in the tumor environment (for example, due to pharmacokinetic reasons). However, the results collected *in vivo*, discussed below, are promising, being associated with a higher bioactivity.

In vivo studies

The acute toxicity of the compounds investigated in this study was preliminarily assessed using the fish embryo acute toxicity (FET) test on zebrafish (*Danio rerio*) embryos, monitored up to 96 hours post-fertilization (hpf).

Zebrafish (ZF) is a teleost fish that exhibits highly conserved physiological pathways among vertebrates, with approximately 70% of homology to human genes.[60] The FET test has been considered so far for a large class of compounds associated with various different mechanisms of action, volatility, solubility and hydrophobicity.[61,62]

The choice of the ZF model in toxicological research is due to a number of advantages, such as cost-effectiveness (also associated with its small size), easy maintenance, huge egg production during the year (a single female can yield 50–200 eggs per day) and rapid development. Embryos undergo complete development within 96 hours at 26 ± 1 °C and achieve maturity within three months, making them an ideal choice for both laboratory research and eco-toxicological testing.

In the FET assay, twenty newly fertilized eggs per concentration are exposed to the test substance for a period of 96 hpf so as to determine the LC_{50} value, the concentration at which 50% of the embryos do not survive, or show sub-lethal effects, under the considered conditions.

In this work, the two quinolines **8AQ** and **8NQ** were studied individually to first evaluate their toxicity, followed by the FET test of **8AQ** in the presence of copper. Copper(II) chloride alone was tested, showing high toxicity towards the embryos with an LC_{50} = 0.97 μM (95% limits: 0.85–1.05 μM). No sub-lethal effects were found but only lethal effects (death of embryos) and developmental delays.

8NQ was tested *in vivo* at the concentrations 28, 50, 100, 200 and 500 μM. Embryos were observed over 4 days, recording lethal endpoints and sublethal toxicity. At the highest tested concentrations, all embryos were coagulated. At subsequent dilutions, the observed effects were malformation of the tail and other coagulation phenomena.

At the concentrations of 50 and 100 μM, a delay in development (up to 144 h) was observed in most individuals, while at 50, 100 and 200 μM, depigmentation phenomena were clearly visible (Fig. 3). In alignment with *in vitro* results, **8NQ** demonstrated lower toxicity [LC_{50} = 171.1 μM (95% limits: 143.1–180.5 μM)] compared to its amino counterpart, **8AQ** [LC_{50} = 19.49 μM (95% limits: 16.43–23.99 μM)].

The ligand **8AQ** in the absence of copper ions was tested *in vivo* at the concentrations of 5, 10, 25, 40 and 50 μM. Embryos were observed over 4 days, recording lethal endpoints and sub-lethal toxicity. At the highest tested concentrations, the observed effects were coagulation phenomena after the first 24 hours in 8 embryos and death in all the remaining formed embryos at the end of the test (Fig. 4). At the two lowest concentrations, only coagulation phenomena were observed.

With regard to the system formed *in situ* by complexation of copper by **8AQ**, the LC_{50} parameter decreases to 12.6 μM in terms of **8AQ** concentration (in the presence of copper). This confirms the increase in the toxicity of **8AQ** upon coordination to the transition metal center [LC_{50} achieved at a copper concentration of 3.7 μM (95% limits: 3.39–4.16 μM)]. Fig. 5 shows indeed the effects observed at comparable **8AQ** concentrations, in the absence of copper (10 μM; Fig. 5A) and in the presence of copper (13.6 μM **8AQ** [4 μM of $CuCl_2$] Fig. 5B), recording a development delay, similar to subsequent dilutions (detected only in a few cases). At higher **8AQ** concentrations (34 μM, combined with $CuCl_2$ at 10 μM), most embryos were dead while the remaining embryos, although hatched, showed a bradycardic heartbeat and no movement.

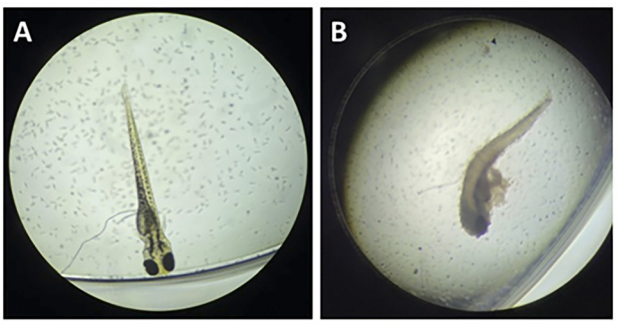

Fig. 4 Images of zebrafish embryos treated with **8AQ**. The negative control showed normal pigmentation at 96 hpf (A). Dead zebrafish embryo treated with the highest concentration (50 μM) of **8AQ** (B).

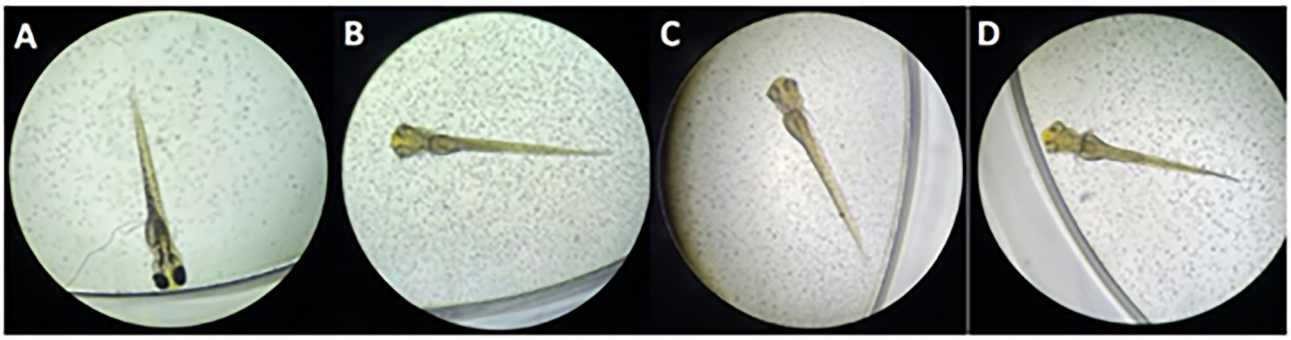

Fig. 3 Images of zebrafish embryos treated with **8NQ**. The negative control showed normal pigmentation at 96 hpf (A). The embryos treated with **8NQ** at concentrations of 50 μM (B), 100 μM (C), and 200 μM (D) showed depigmentation at 96 hpf.

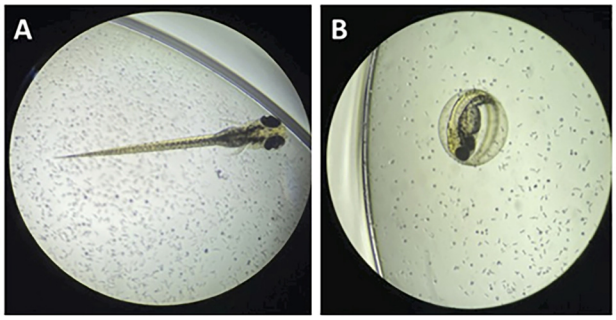

Fig. 5 Images of zebrafish embryos treated with **8AQ** and the system formed *in situ* by complexation of **8AQ** with Cu^{2+}. Zebrafish treated with **8AQ** at 10 μM (A); and zebrafish exhibiting delayed development after treatment with **8AQ** (13.6 μM) and $CuCl_2$ (4 μM) (B).

To sum up, **8NQ** is the less toxic compound, followed by **8AQ**. Once combined with copper, **8AQ** proved to be more toxic, consistent with the higher cytotoxicity recorded *in vitro*.

Experimental

Chemicals and materials

Commercially available reagents/solvents, including 3-(*N*-morpholino)propanesulfonic acid (MOPS), sterile dimethyl sulfoxide (DMSO), 3-(4,5-dimethylthiazol-2-yl)-2,5-diphenyltetrazolium bromide (MTT), glutathione (GSH), fetal bovine serum (FBS), $CuCl_2$ dihydrate, *n*-octanol, **8NQ** and **8AQ** were purchased from Merck. DMEM (Dulbecco's modified Eagle's medium) w/GlutaMAX™-I (pyruvate 1 mM) cell growth medium, an antibiotic mixture of penicillin and streptomycin (10 000 U mL^{-1}), MEM non-essential amino acid solution (100×), and phosphate-buffered saline (PBS) were purchased from Thermo Fisher Life Technologies. MEM (minimum essential medium) was purchased from Euroclone. All chemicals were high-grade and used as purchased without further purification. Stock solutions of Cu^{2+} were prepared by dissolving the corresponding perchlorate salt in water. The resulting solutions were then titrated with standardized EDTA.

Log *P*

The *n*-octanol/water partition coefficient (log *P*) was defined using the corresponding bi-phasic solvent system, widely considered by the scientific community since it well mimics the water/phospholipid membrane interface. The compounds were dissolved in *n*-octanol (achieving mM concentrations), followed by dilution at an appropriate concentration (25 μM for **8AQ** and 250 μM for **8NQ**) in the same alcohol. A defined volume was added to water (same volume), and the resulting mixture was stirred at 25 °C overnight. After partitioning, all mixtures were left to equilibrate for 4 hours. The concentrations of the compounds in the two phases after equilibration were identified using a Jasco V-730 UV-Vis spectrophotometer (double beam) in the wavelength range of 250–500 nm (λ_{8AQ} = 252 nm; λ_{8NQ} = 313 nm).

The final log *P* values, reported as mean ± SD of at least three independent measurements, were calculated according to the equation $\log P = \log[A1/(A0 - A1)]$, where $A0$ is the absorbance (proportional to the initial concentration) of the compound in *n*-octanol before partitioning into water, and $A1$ is the absorbance (proportional to the final concentration) of the compound under examination in *n*-octanol after partitioning at the considered wavelength.

Mass spectrometry

Electrospray ionization mass spectrometry (ESI-MS) was conducted on copper complexes, prepared by adding a solution of Cu^{2+} to an aqueous solution of the ligand. The pH value was adjusted using a stock solution of NaOH, to avoid the presence of high amounts of salts that could interfere with the ionization process. Stock solutions of **8AQ** and **8NQ** were freshly prepared at 0.02 M by dissolving a weighed amount of each compound in ethanol. Different metal/ligand ratios were investigated. An excess of Cu^{2+} was also used in the case of **8NQ**. The MS parameters were optimized for improved signal responses.

Mass spectral analysis and assignment were carried out using the Xcalibur software, with each species labelled with the *m*/*z* value of the first peak in its isotopic cluster.

UV-Vis spectrophotometry

UV-Vis spectra were obtained using a JASCO V-670 spectrophotometer. Spectrophotometric titrations were conducted in a MOPS buffer (0.01 M)/ethanol 70 : 30 v/v solution at pH 7.4. The metal complexes of **8AQ** were less soluble than the ligand and the addition of an organic solvent (ethanol) was necessary to prevent the formation of precipitates.

Cell culture

A549 and HCT116 human cancer cell lines were obtained from American Type Culture Collection (Manassas, VA) and HepG2 cells were obtained from DIMED, University of Padova (Padova, Italy). A549 and HCT116 were grown in DMEM supplemented with 10% FBS while HepG2 cells were grown in MEM supplemented with 15% FBS and 1% MEM non-essential amino acids. Cells were grown in a humidified incubator at 37 °C with 5% CO_2.

Cell viability assays

The compounds under investigation along with the combination of Cu^{2+}–**8AQ** and Cu^{2+}–**8NQ** were evaluated in terms of cytotoxic activity *in vitro* using the MTT test.[63] Cells were seeded in 96-well plates (1×10^4 cells per well for HepG2 and HCT116; 7×10^3 cells per well for A549), followed by treatment with **8NQ**, **8AQ** or their combination with Cu^{2+}. After 72 h of incubation at 37 °C, the cells were washed with PBS and then incubated with 0.5 mg mL^{-1} MTT for 3 h at 37 °C. Afterward, 100 μL of stop solution (90% isopropanol/10% DMSO) was added, and 15 min later, the absorbance (Abs) at 595 and 690 nm was estimated. The Infinite M Plex (TECAN) UV-Vis spectrophotometer was used for the spectrophotometric reading of 96-well plates.

The biological activity of the compounds was quantified as the percentage of surviving cells compared to untreated cells. For each sample, the concentration required to induce 50% death of the tumour cell population compared to the control (EC_{50}) was evaluated. At least four MTT tests for each compound were carried out in order to evaluate the corresponding EC_{50} values.

In vivo studies

The fish embryo acute toxicity (FET) tests were carried out according to the Organization for Economic Co-operation and Development (OECD) guidelines for chemical testing (test no.236).[64] All experiments were performed in compliance with the relevant laws and institutional guidelines: at the embryonic stages used in the FET test, zebrafish embryos are not considered as experimental animals under European legislation (Directive 2010/63/EU of the European Parliament and of the Council of 22 September 2010 on the protection of animals used for scientific purposes Text with EEA relevance). These testing guidelines are related to the acute toxicity of substances using ZF embryos up to 96 hours post-fertilization.

The model organisms [supplied by the ZF Facility of the University of Padova (Italy)], kept in saline water (the composition of which is described below) at a constant temperature of 26 ± 1 °C during the whole test, were observed every 24 hours, considering the following four indicators of lethality: (I) coagulation of fertilised eggs. Even with no magnification, coagulated eggs can be clearly identified: they are milky white. Under the microscope, they look dark. The number of coagulated embryos is determined after 24, 48, 72 and 96 h. (II) Lack of somite formation. At 26 ± 1 °C, around 20 somites form after 24 h in a normally developing ZF embryo. A healthy embryo shows spontaneous movements (side-to-side contractions), which are related to somite formation. The absence of somites is recorded after 24, 48, 72 and 96 h. (III) Lack of heartbeat. In a normally developing ZF embryo at 26 ± 1 °C, the heartbeat is visible after 48 h. The absence of heartbeat is recorded after 48, 72 and 96 h. (IV) Absence of tail detachment (recordable after 24, 48, 72 and 96 h) from the yolk sac. In a normal ZF embryo, detachment of the tail-bud from the yolk is observed after posterior elongation of the embryonic body. Other reportable sublethal effects are depigmentation and delay of development.

At the end of the exposure period, acute toxicity was determined based on a positive outcome in any of the four endpoint observations. The test time period was 96 hours, followed by the LC_{50} calculation. The lethal concentration value (LC_{50}) was estimated with its 95% confidence limits using a statistical program that uses the Probit method for calculation (PROBIFS).[65]

Appropriate ZF water (294.0 mg L^{-1} $CaCl_2{\cdot}2H_2O$; 123.3 mg L^{-1} $MgSO_4{\cdot}7H_2O$; 64.7 mg L^{-1} $NaHCO_3$; 5.7 mg L^{-1} KCl) was prepared according to the OECD guidelines[61,62] and was used both as a negative control and for dilutions. An additional negative control was considered, containing the solubilizing agent DMSO (0.5% v/v), used in stock solution preparation. When an organic solvent is used, it should produce no adverse effect on the embryos as checked by the solvent control; mortality in solvent control should be <20%. The overall survival of embryos in the negative control and the solvent control should be ≥80% until hatch.[64]

As a positive control, three concentrations (2.5 mg L^{-1}; 5 mg L^{-1}; and 10 mg L^{-1}) of 3,4-dichloroaniline were prepared in dilution water.[66,67]

After weighing, stock solutions of both quinolines were prepared by dissolution in DMSO to yield millimolar concentrations while copper(II) chloride dihydrate was solubilized in ZF water. Each final concentration of all samples was obtained, starting from stock solutions, by dissolving the test compounds in a total volume of 200 mL of dilution water.

The ionophore precursor **8NQ** was tested at the concentrations 28, 50, 100, 200 and 500 μM. **8AQ** alone and in combination with copper chloride was evaluated at 10, 25, 40 and 50 μM and at 34, 13.6, 6.8, 3.4 and 0.034 μM, respectively. Regarding the latter, the *in situ* metal–ligand complexation was tested by solubilizing the ionophore **8AQ** together with Cu^{2+} in the form of cupric chloride dihydrate (10, 4, 2, 1 and 0.01 μM). $CuCl_2{\cdot}2H_2O$ alone was tested at the concentrations 10, 7, 3.5, 1 and 0.1 μM.

Compound exposure was such that ± 20% of the nominal chemical concentration was maintained throughout the test. A semi-static renewal interval was applied (renewal every 24 h).[64]

Conclusions

This study provides new insights into the potential of 8-aminoquinoline (**8AQ**) as an anticancer agent in the presence of copper ions. While **8AQ** alone exhibits limited cytotoxicity against the tested human cancer cell lines (A549, HepG2 and HCT116), its combination with copper significantly enhances its efficacy, highlighting a promising synergistic effect.

Our findings reinforce the emerging relevance of copper-based chemotherapeutic strategies. **8AQ** may act as an ionophore, transporting copper into tumor cells where it is released upon interaction with intracellular glutathione, leading to copper overload. This mechanism, consistent with known 8HQ-based ionophores, is associated with cell death induction by causing copper dyshomeostasis in cancer cells.

This study introduced the zebrafish model for the evaluation of copper-based systems for oncological applications. This model validated the *in vitro* results and the Cu^{2+}–**8AQ** system emerges as a viable candidate for further preclinical evaluation, offering a promising avenue for the rational design of next-generation metal-based anticancer agents with improved selectivity and therapeutic index.

Author contributions

A. S. and E. M. contributed to the determination of the log *P* values of the compounds and to the cellular assays on A549

cells. R. P. and G. P. contributed to both *in vitro* cell-based experiments and *in vivo* measurements. M. L. and R. C. coordinated and supervised *in vivo* experiments, followed by data processing. L. C. contributed to the study of the interaction between the complexes and glutathione (GSH). G. A. and V. S. performed the *in vitro* assays on HCT116 and HepG2 cell lines. C. N. conceived the study in collaboration with V. O., coordinated the experimental *in vitro* and *in vivo* evaluations, contributed to manuscript preparation, and was involved in securing funding for the project. V. O. conceived the study with C. N., coordinated the research activities investigating the copper complexes and their interaction with GSH, wrote the manuscript and financially supported this work. All authors have read and agreed to the published version of the manuscript.

Conflicts of interest

There are no conflicts to declare.

Data availability

The data supporting this article have been included as part of the SI. SI contains ESI-MS spectra and isotopic pattern simultations of the copper complexes species of 8AQ and the mixture GSH-Cu-8AQ; UV-vis titration of 8AQ-Cu^{2+} with DMEM. See DOI: **https://doi.org/10.1039/d5dt01396h**.

Acknowledgements

This work was carried out as part of the PRIN2022 project (no. 2022BTMYWZ; CUP code: B53D23015260006) entitled "New mEtal-baSed agenTs against Orphan tumoRs – NESTOR" [announcement D.D. 104 del 02/02/2022 - PNRR per la Missione 4, Componente 2, Investimento 1.1], financed by the European Union – NextGenerationEU". CN is grateful to the EU for the financial support by the "HEAL ITALIA" PE6 (Partenariato Esteso 6) project [PNRR European Union funds - Missione 4, Componente 2, Investimento 1.3 - CUP B33C22001030006]. L. C. and V. O. also thank the University of Catania (Starting Grant Project: SELECTION and Piaceri 2024: TRACE). M. L. and R. C. are grateful to Agrolab Italia for supporting this academia–company project and to Edoardo Zanolla for technical support in the last part of this work.

References

1 F. B. Ahmad, J. A. Cisewski and R. N. Anderson, *J. Am. Med. Assoc.*, 2024, **332**, 957–958.
2 S. Mubarik, L. Luo, S. Naeem, R. Mubarak, M. Iqbal, E. Hak and C. Yu, *Public Health*, 2024, **231**, 187–197.
3 B. Liu, H. Zhou, L. Tan, K. T. H. Siu and X.-Y. Guan, *Signal Transduction Targeted Ther.*, 2024, **9**, 175.
4 A. Zafar, M. J. Khan, J. Abu and A. Naeem, *Mol. Biol. Rep.*, 2024, **51**, 219.
5 G. S. França, M. Baron, B. R. King, J. P. Bossowski, A. Bjornberg, M. Pour, A. Rao, A. S. Patel, S. Misirlioglu, D. Barkley, K. H. Tang, I. Dolgalev, D. A. Liberman, G. Avital, F. Kuperwaser, M. Chiodin, D. A. Levine, T. Papagiannakopoulos, A. Marusyk, T. Lionnet and I. Yanai, *Nature*, 2024, **631**, 876–883.
6 H. Fatma and H. R. Siddique, *Cancer Metastasis Rev.*, 2024, **43**, 423–440.
7 A. Valente, A. Podolski-Renić, I. Poetsch, N. Filipović, Ó. López, I. Turel and P. Heffeter, *Drug Resistance Updates*, 2021, **58**, 100778.
8 S. Abdolmaleki, A. Aliabadi and S. Khaksar, *Coord. Chem. Rev.*, 2024, **501**, 215579.
9 V. Oliveri, *Front. Mol. Biosci.*, 2022, **9**, 1–14.
10 L. Aubert, N. Nandagopal, Z. Steinhart, G. Lavoie, S. Nourreddine, J. Berman, M. K. Saba-El-Leil, D. Papadopoli, S. Lin, T. Hart, G. Macleod, I. Topisirovic, L. Gaboury, C. J. Fahrni, D. Schramek, S. Meloche, S. Angers and P. P. Roux, *Nat. Commun.*, 2020, **11**, 3701.
11 A. K. Baltaci, T. K. Dundar, F. Aksoy and R. Mogulkoc, *Biol. Trace Elem. Res.*, 2017, **175**, 57–64.
12 M. Stepien, M. Jenab, H. Freisling, N. P. Becker, M. Czuban, A. Tjønneland, A. Olsen, K. Overvad, M. C. Boutron-Ruault, F. R. Mancini, I. Savoye, V. Katzke, T. Kühn, H. Boeing, K. Iqbal, A. Trichopoulou, C. Bamia, P. Orfanos, D. Palli, S. Sieri, R. Tumino, A. Naccarati, S. Panico, H. B. Bueno-de-Mesquita, P. H. Peeters, E. Weiderpass, S. Merino, P. Jakszyn, M. J. Sanchez, M. Dorronsoro, J. M. Huerta, A. Barricarte, S. Boden, B. van Guelpen, N. Wareham, K. T. Khaw, K. E. Bradbury, A. J. Cross, L. Schomburg and D. J. Hughes, *Carcinogenesis*, 2017, **38**, 699–707.
13 A. Gupte and R. J. Mumper, *Cancer Treat. Rev.*, 2009, **35**, 32–46.
14 E. J. Ge, A. I. Bush, A. Casini, P. A. Cobine, J. R. Cross, G. M. DeNicola, Q. P. Dou, K. J. Franz, V. M. Gohil, S. Gupta, S. G. Kaler, S. Lutsenko, V. Mittal, M. J. Petris, R. Polishchuk, M. Ralle, M. L. Schilsky, N. K. Tonks, L. T. Vahdat, L. Van Aelst, D. Xi, P. Yuan, D. C. Brady and C. J. Chang, *Nat. Rev. Cancer*, 2022, **22**, 102–113.
15 Z. J. Wang, Q. W. Guan, H. H. Zhou, X. Y. Mao and F. H. Chen, *Genes Dis.*, 2023, **10**, 771–785.
16 J. Li, X. Wang, R. Liu, J. Zi, Y. Li, Z. Li and W. Xiong, *J. Cancer*, 2024, **15**, 5230–5243.
17 D. Tang, G. Kroemer and R. Kang, *Nat. Rev. Clin Oncol.*, 2024, **21**, 370–388.
18 P. Tsvetkov, S. Coy, B. Petrova, M. Dreishpoon, A. Verma, M. Abdusamad, J. Rossen, L. Joesch-Cohen, R. Humeidi, R. D. Spangler, J. K. Eaton, E. Frenkel, M. Kocak, S. M. Corsello, S. Lutsenko, N. Kanarek, S. Santagata and T. R. Golub, *Science*, 2022, **375**, 1254–1261.
19 P. A. Cobine and D. C. Brady, *Mol. Cell*, 2022, **82**, 1786–1787.

20 Q. Lou, F. Lai, J. Li, K. Mao, H. Wan and Y. He, *Apoptosis*, 2024, **29**, 981–1006.
21 D. Denoyer, S. Masaldan, S. La Fontaine and M. A. Cater, *Metallomics*, 2015, **7**, 1459–1476.
22 V. Oliveri, *Coord. Chem. Rev.*, 2020, **422**, 213474.
23 V. Oliveri, V. Lanza, D. Milardi, M. Viale, I. Maric, C. Sgarlata and G. Vecchio, *Metallomics*, 2017, **9**, 1439–1446.
24 V. Oliveri and G. Vecchio, *J. Inorg. Biochem.*, 2016, **162**, 31–43.
25 V. Oliveri, *ChemistryOpen*, 2015, **4**, 792–795.
26 N. Pettenuzzo, L. Brustolin, E. Coltri, A. Gambalunga, F. Chiara, A. Trevisan, B. Biondi, C. Nardon and D. Fregona, *ChemMedChem*, 2019, **14**, 1162–1172.
27 M. Celegato, D. Fregona, M. Mongiat, L. Ronconi, C. Borghese, V. Canzonieri, N. Casagrande, C. Nardon, A. Colombatti and D. Aldinucci, *Future Med. Chem.*, 2014, **6**, 1249–1263.
28 B. Shang, Z. Yu and Z. Wang, *Front. Pharmacol.*, 2024, **15**, 1–9.
29 F. B. Palmer, C. A. Butler, M. H. Timperley and C. W. Evans, *Environ. Toxicol. Chem.*, 1998, **17**, 1538–1545.
30 J. K. Fraser, C. A. Butler, M. H. Timperley and C. W. Evans, *Environ. Toxicol. Chem.*, 2000, **19**, 1397–1402.
31 L. D. Grünspan, B. H. M. Mussulini, S. Baggio, P. R. Dos Santos, F. Dumas, E. P. Rico, D. L. de Oliveira and S. Moura, *Epilepsy Res.*, 2018, **139**, 171–179.
32 S. Zhang, D. R. Sadhasivam, S. Soundarajan, P. Shanmugavel, A. Raji and M. Xu, *3 Biotech*, 2023, **13**, 45.
33 D. C. Kanellis, A. Zisi, Z. Skrott, B. Lemmens, J. A. Espinoza, M. Kosar, A. Björkman, X. Li, S. Arampatzis, J. Bartkova and M. Andújar-Sánchez, *Cell Death Differ.*, 2023, **30**, 1666–1678.
34 H. Draut, T. Rehm, G. Begemann and R. Schobert, *Chem. Biodivers.*, 2017, **14**, e1600302.
35 V. Virtanen and M. Karonen, *Molecules*, 2020, **25**, 3691.
36 A. Elgendy and A. Adejare, *Int. J. Appl. Pharm.*, 2024, **16**, 1–6.
37 L. Brustolin, C. Nardon, N. Pettenuzzo, N. Zuin Fantoni, S. Quarta, F. Chiara, A. Gambalunga, A. Trevisan, L. Marchiò, P. Pontisso and D. Fregona, *Dalton Trans.*, 2018, **47**, 15477–15486.
38 O. Mazuryk, K. Magiera, B. Rys, F. Suzenet, C. Kieda and M. Brindell, *JBIC, J. Biol. Inorg. Chem.*, 2014, **19**, 1305–1316.
39 G. Pastuch-Gawołek and J. Szreder, *Molecules*, 2025, **30**, 427.
40 M. K. Paira, J. Dinda, T.-H. Lu, A. R. Paital and C. Sinha, *Polyhedron*, 2007, **26**, 4131–4140.
41 R. M. Smith and A. E. Martell, *Critical stability constants: volume 2: amines*, Springer, 1975.
42 M. Mirzaei, H. Eshtiagh-Hosseini, Z. Bolouri, Z. Rahmati, A. Esmaeilzadeh, A. Hassanpoor, A. Bauza, P. Ballester, M. Barceló-Oliver, J. T. Mague and B. Notash, *Cryst. Growth Des.*, 2015, **15**, 1351–1361.
43 V. Arjunan, P. Ravindran, T. Rani and S. Mohan, *J. Mol. Struct.*, 2011, **988**, 91–101.
44 S. C. Lu, *Biochim. Biophys. Acta, Gen. Subj.*, 2013, **1830**, 3143–3153.
45 M. Jozefczak, T. Remans, J. Vangronsveld and A. Cuypers, *Int. J. Mol. Sci.*, 2012, **13**, 3145–3175.
46 D. A. Averill-Bates, *Vitamins and hormones*, Academic Press, 2023, vol. 121, pp. 109–141.
47 F. Q. Schafer and G. R. Buettner, *Free Radicals Biol. Med.*, 2001, **30**, 1191–1212.
48 E. Hatem, N. El Banna and M.-E. Huang, *Antioxid. Redox Signal.*, 2017, **27**, 1217–1234.
49 D. M. Townsend, K. D. Tew and H. Tapiero, *Biomed. Pharmacother.*, 2003, **57**, 145–155.
50 J. Liu, H. Tang, F. Chen, C. Li, Y. Xie, R. Kang and D. Tang, *Sci. Rep.*, 2024, **14**, 29579.
51 H. Speisky, M. Gómez, F. Burgos-Bravo, C. López-Alarcón, C. Jullian, C. Olea-Azar and M. E. Aliaga, *Bioorg. Med. Chem.*, 2009, **17**, 1803–1810.
52 E. Cadoni, E. Valletta, G. Caddeo, F. Isaia, M. G. Cabiddu, S. Vascellari and T. Pivetta, *J. Inorg. Biochem.*, 2017, **173**, 126–133.
53 M. Ebara, H. Fukuda, R. Hatano, M. Yoshikawa, N. Sugiura, H. Saisho, F. Kondo and M. Yukawa, *Oncology*, 2003, **65**, 323–330.
54 M. Ebara, H. Fukuda, R. Hatano, H. Saisho, Y. Nagato, K. Suzuki, K. Nakajima, M. Yukawa, F. Kondo, A. Nakayama and H. Sakurai, *J. Hepatol.*, 2000, **33**, 415–422.
55 M. O. Song, J. Li and J. H. Freedman, *Physiol. Genomics*, 2009, **38**, 386–401.
56 N. Arnal, M. J. T. De Alaniz and C. A. Marra, *Hum. Exp. Toxicol.*, 2013, **32**, 299–315.
57 D. Yang, H. Y. Tian, T. N. Zang, M. Li, Y. Zhou and J. F. Zhang, *Sci. Rep.*, 2017, **7**, 9174.
58 Y. Li, Y. Sun, J. Li, Q. Su, W. Yuan, Y. Dai, C. Han, Q. Wang, W. Feng and F. Li, *J. Am. Chem. Soc.*, 2015, **137**, 6407–6416.
59 K. Li, Y. Sun, Z. Ma, Y. Chen, X. Li, G. Dong, D. Liu, C. Sheng and S. Wu, *J. Med. Chem.*, 2025, **68**, 12402–12413.
60 K. Howe, M. D. Clark, C. F. Torroja, J. Torrance, C. Berthelot, M. Muffato, J. E. Collins, S. Humphray, K. McLaren, L. Matthews, S. McLaren, I. Sealy, M. Caccamo, C. Churcher, C. Scott, J. C. Barrett, R. Koch, G. J. Rauch, S. White, W. Chow, *et al.*, *Nature*, 2013, **496**, 498–503.
61 OECD GD 23, *Guidance Document on Aqueous-Phase Aquatic Toxicity Testing of Difficult Test Chemicals*, Organisation for Economic Co-operation and Development, Paris, 2nd edn, 2018.
62 OECD GD 29, *Guidance Document on Transformation/Dissolution of Metals and Metal Compounds in Aqueous Media*, Organisation for Economic Co-operation and Development, Paris, 2nd edn, 2002.
63 J. van Meerloo, G. J. L. Kaspers and J. Cloos, Cell sensitivity assays: the MTT assay, in *Cancer cell culture*, ed. I. A. Cree, Humana Press, New York, 2011, pp. 237–245.

64 OECD, *Test No. 236: Fish Embryo Acute Toxicity (FET) Test, OECD Guidelines for the Testing of Chemicals, Section 2*, OECD Publishing, Paris, 2013.
65 A. Puddu, *Metodi analitici per le acque. Notiziario CNR-IRSA*, 1989, **9**, 19–37.
66 OECD, *Validation Report (Phase 1) for the Zebrafish Embryo Toxicity Test: Part I and Part II. Series on Testing and Assessment No. 157*, OECD, Paris, 2011.
67 OECD, *Validation Report (Phase 2) for the Zebrafish Embryo Toxicity Test: Part I and Part II (Annexes). Series on Testing and Assessment No. 179*, OECD, Paris, 2012.